

Appendix A: TPFs

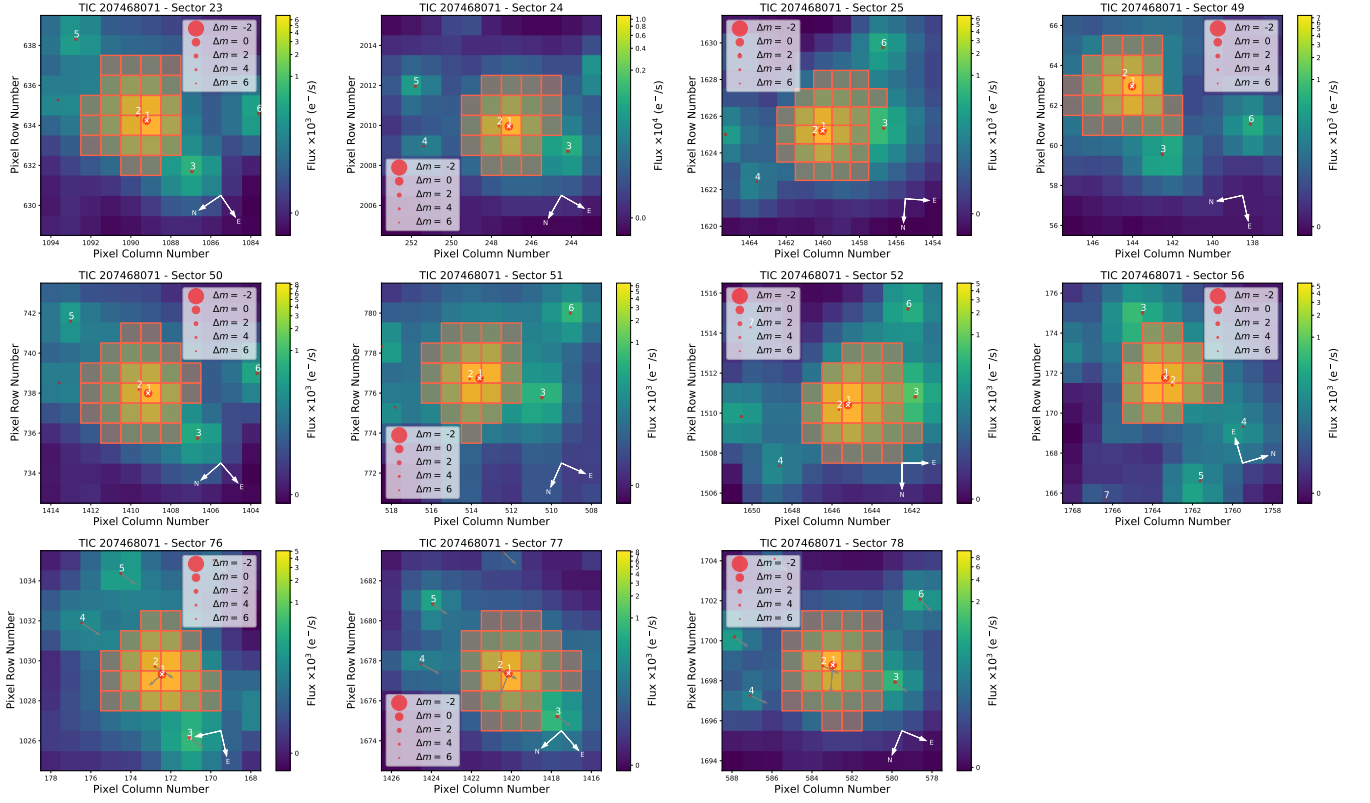


Fig. A.1: The TPFs for TOI-1836, created by `tpfplotter` (Aller et al. 2020). The images display electron counts, with the SPOC aperture mask outlined in red. Red circles are used to indicate the primary target (marked as 1) and nearby sources (rest of the numbers) based on their positions in Gaia DR3. The size of these circles corresponds to the relative magnitudes of the sources compared to the target star. Additionally, arrows illustrate the proper motion of each star.

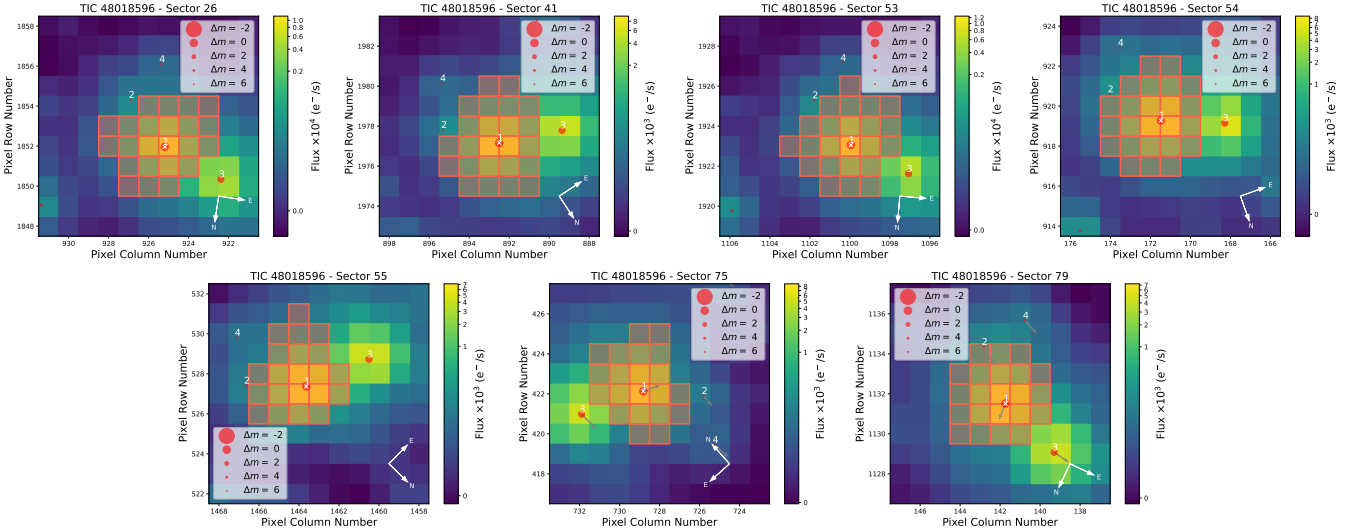


Fig. A.2: The TPFs for TOI-2295. Same as the caption of Fig. A.1

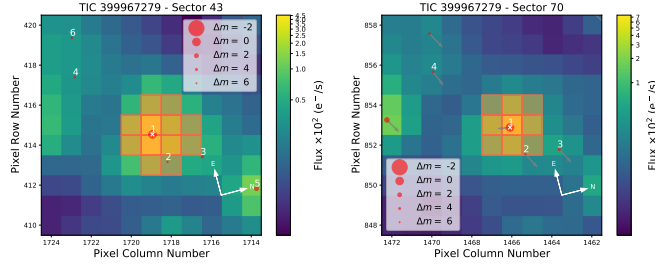


Fig. A.3: The TPFs for TOI-2537. Same as the caption of Fig. A.1

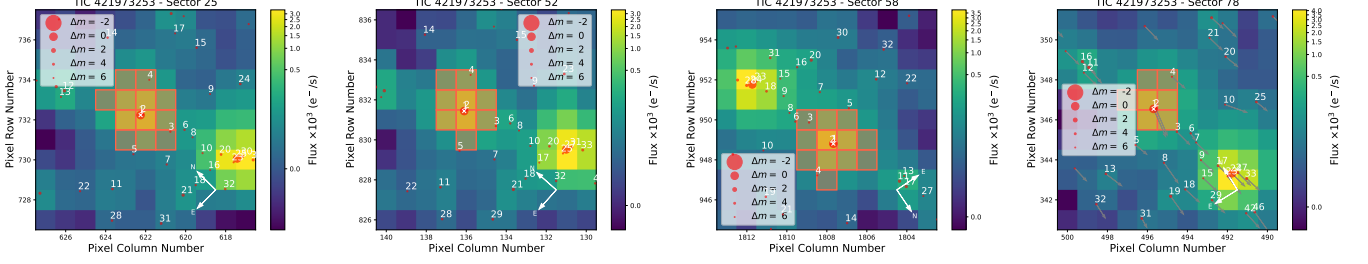


Fig. A.4: The TPFs for TOI-4081. See the caption of Fig. A.1 for more explanation.

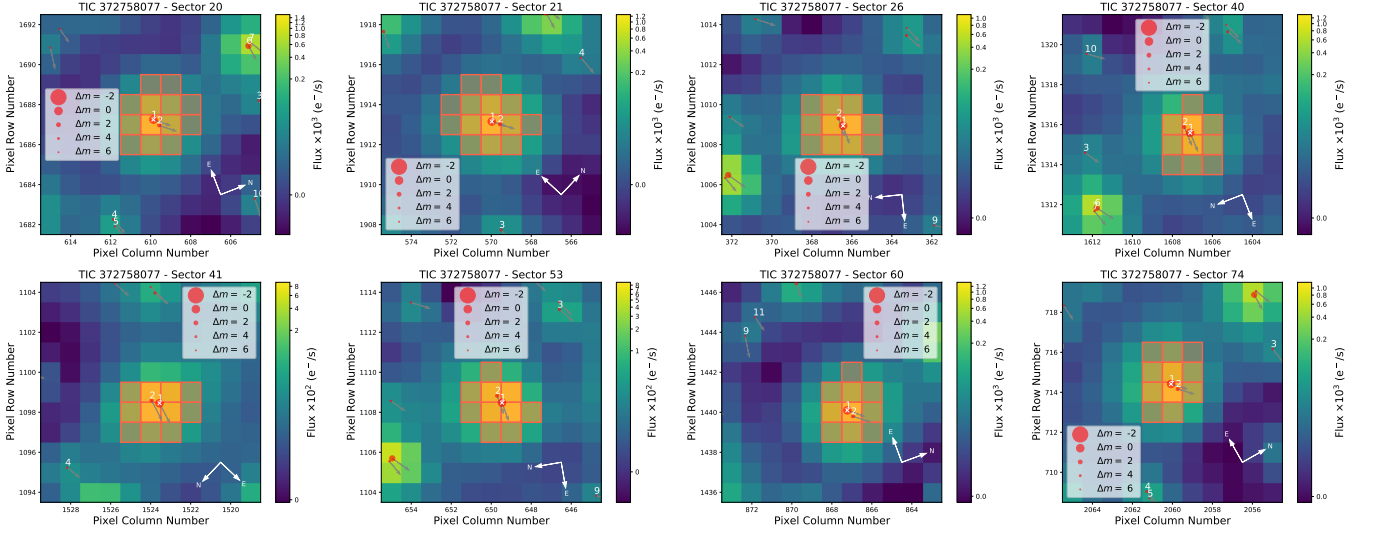


Fig. A.5: The TPFs for TOI-4168. See the caption of Fig. A.1 for more explanation.

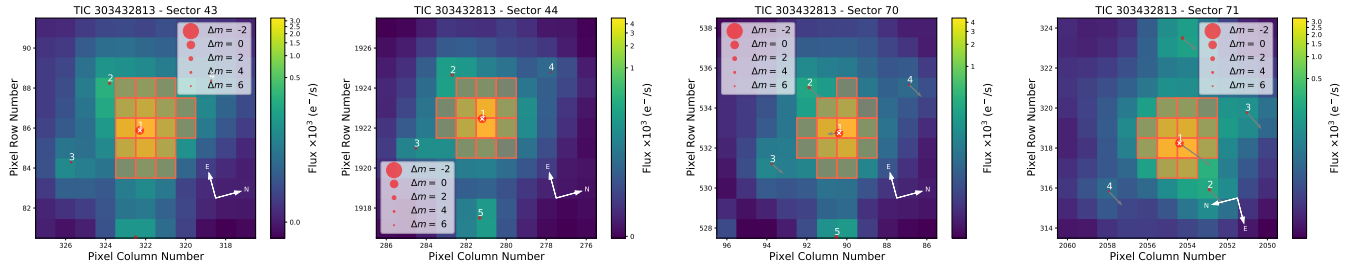


Fig. A.6: The TPFs for TOI-5076. See the caption of Fig. A.1 for more explanation.

Appendix B: RVs

In this section, we present the RVs used in this study. We note that the bisector error bars are considered to be twice the RV uncertainties.

Table B.1: SOPHIE RVs for TOI-2295.

BJD (-2400000 d)	RV (km s ⁻¹)	σ_{RV} (m s ⁻¹)	BIS (km s ⁻¹)
59130.38267	-38.5705	0.0037	-0.0298
59172.24841	-38.6415	0.0027	-0.022
59197.21288	-38.6371	0.0027	-0.0209
....

Notes. This table is available in its entirety in machine-readable form

Table B.2: SOPHIE RVs for TOI-2537.

BJD (-2400000 d)	RV (km s ⁻¹)	σ_{RV} (m s ⁻¹)	BIS (km s ⁻¹)
58730.59024	61.4184	0.0187	-0.0798
58797.43469	61.5845	0.0178	-0.0342
58813.35391	61.5442	0.0146	-0.118
....

Notes. This table is available in its entirety in machine-readable form

Table B.3: HARPS RVs for TOI-2537.

BJD (-2400000 d)	RV (km s ⁻¹)	σ_{RV} (m s ⁻¹)	BIS (km s ⁻¹)
59225.5762851	61559.300	8.900	18.000
59229.5574822	61555.700	12.700	-7.000
59232.5606435	61568.100	12.700	29.000
....

Notes. This table is available in its entirety in machine-readable form

Table B.4: FEROS RVs for TOI-2537.

BJD (-2400000 d)	RV (km s ⁻¹)	σ_{RV} (m s ⁻¹)	BIS (km s ⁻¹)
59187.6430111	61637.700	10.400	-29.000
59191.6669117	61585.300	10.000	-15.000
59194.6038561	61527.400	10.200	-52.000
....

Notes. This table is available in its entirety in machine-readable form

Table B.5: SOPHIE RVs for TOI-4168.

BJD (-2400000 d)	RV (km s ⁻¹)	σ_{RV} (m s ⁻¹)	BIS (km s ⁻¹)
59562.66417	-48.9584	0.0061	0.0114
59563.68571	-51.3137	0.0063	0.0153
59565.69649	-55.0058	0.0068	-0.0093
....

Notes. This table is available in its entirety in machine-readable form

Table B.6: SOPHIE RVs for TOI-5110.

BJD (-2400000 d)	RV (km s ⁻¹)	σ_{RV} (m s ⁻¹)	BIS (km s ⁻¹)
59626.37719	3.8245	0.0067	0.0419
59683.33134	4.2203	0.0063	0.0319
59687.35537	3.8503	0.0085	0.0421
....

Notes. This table is available in its entirety in machine-readable form

Table B.7: SOPHIE RVs for TOI-5076.

BJD (-2400000 d)	RV (km s ⁻¹)	σ_{RV} (m s ⁻¹)	BIS (km s ⁻¹)
59648.33296	70.3026	0.0052	-0.0097
59803.61773	70.2845	0.0043	-0.0196
59815.60996	70.27	0.0033	0.0107
....

Notes. This table is available in its entirety in machine-readable form

Table B.8: SOPHIE RVs for TOI-1836.

BJD (-2400000 d)	RV (km s ⁻¹)	σ_{RV} (m s ⁻¹)	BIS (km s ⁻¹)
59060.42881	-50.4057	0.0054	0.0386
59112.30495	-50.3635	0.0064	0.025
59114.3336	-50.3784	0.008	0.0089
....

Notes. This table is available in its entirety in machine-readable form

Table B.9: SOPHIE RVs for TOI-4081.

BJD (-2400000 d)	RV (km s ⁻¹)	σ_{RV} (m s ⁻¹)	BIS (km s ⁻¹)
59454.557	-15.1026	0.0316	-0.3034
59455.60477	-14.8966	0.03	-0.1224
59456.6159	-14.8183	0.0292	-0.8567
....

Notes. This table is available in its entirety in machine-readable form

Appendix C: Ground-based light curves

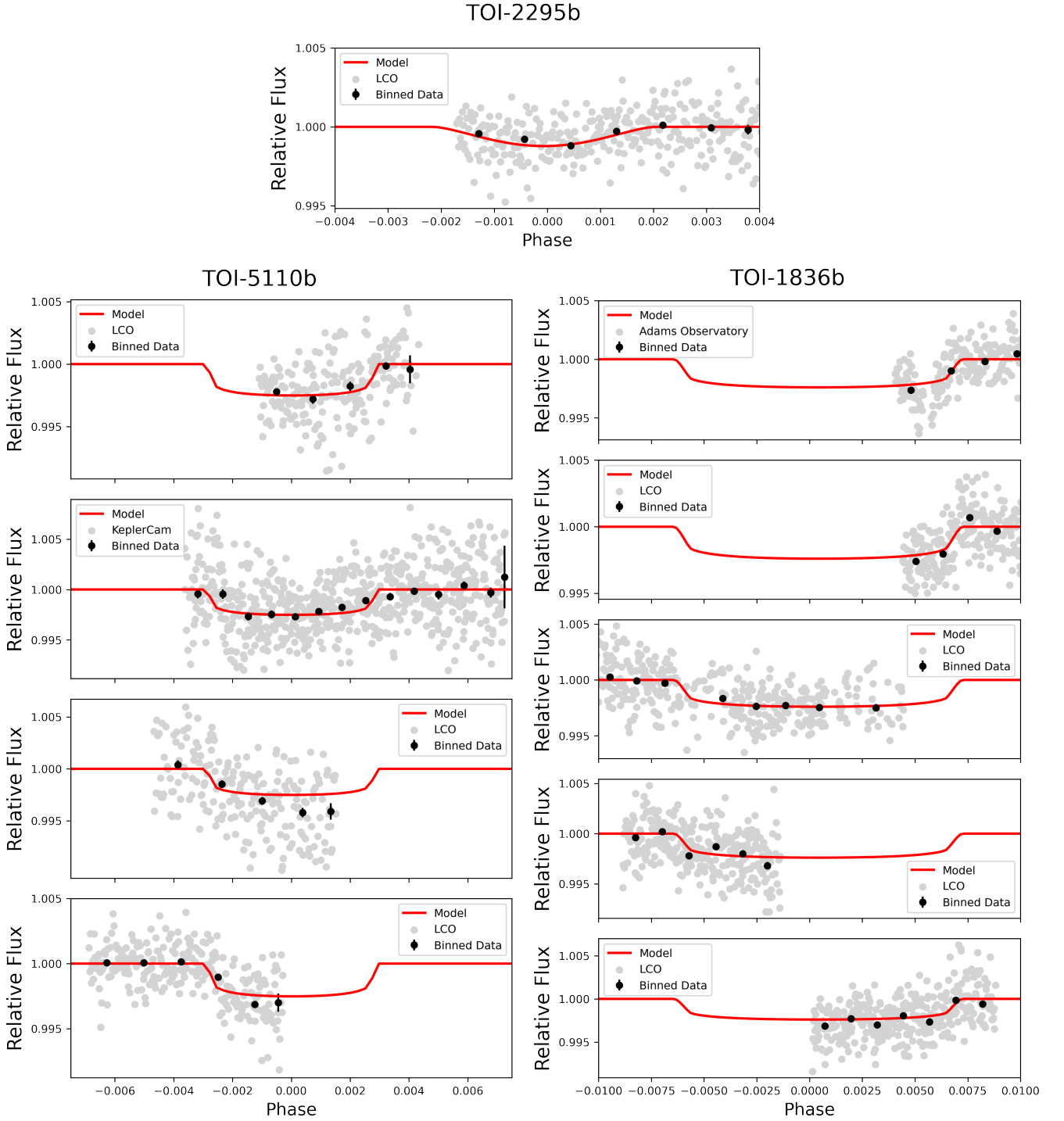


Fig. C.1: Phase-folded ground-based light curves of TOI-2295b, TOI-5110b, and TOI-1836 are shown as gray points. These data are not included in the modeling. The solid red line represents the median model based on the TESS light curve. The data points are binned with a bin size of ~ 0.001 phase.

Appendix D: Priors on RV-only models and joint analysis

Table D.1: Priors and description of parameters used within juliet for RV-only models.

Parameters	Units	TOI-1836	TOI-2295	TOI-2537	TOI-4081	TOI-4168	TOI-5076	TOI-5110
Planet parameters:								
P	Period (d)	.01		b	.01	B	.01	b
T _c -2400000	Center of transit time (d)	$\mathcal{U}(5, 40)$	$\mathcal{U}(1, 50)$	$\mathcal{U}(1, 170)$	$\mathcal{U}(1, 15)$	$\mathcal{U}(1, 50)$	23.444 (fixed)	$\mathcal{U}(1, 50)$
K	RV semi-amplitude (m/s)	$\mathcal{U}(59630, 59664)$	$\mathcal{U}(58688, 58738)$	$\mathcal{U}(58355, 58525)$	$\mathcal{U}(2459729, 2459743)$	$\mathcal{U}(59380, 59420)$	$\mathcal{U}(60193, 60215)$	$\mathcal{U}(59479, 59529)$
e	Eccentricity	0 (fixed)	$\mathcal{U}(0, 70)$	$\mathcal{U}(0, 200)$	$\mathcal{U}(0, 220)$	$\mathcal{U}(0, 30000)$	$\mathcal{U}(0, 30)$	$\mathcal{U}(0, 300)$
ω	Argument of periastron (degrees)	90 (fixed)	$\mathcal{U}(0, 1)$	$\mathcal{U}(0, 1)$	0 (fixed)	$\mathcal{U}(0, 1)$	0 (fixed)	$\mathcal{U}(0, 1)$
			$\mathcal{U}(0, 360)$	$\mathcal{U}(0, 360)$	90 (fixed)	$\mathcal{U}(0, 360)$	90 (fixed)	$\mathcal{U}(0, 360)$
Second planet parameters:								
P	Period (d)	—	c	c	—	—	—	—
T _c -2400000	Center of transit time (d)	—	$\mathcal{U}(700, 1500)$	$\mathcal{U}(800, 5000)$	—	—	—	—
K	RV semi-amplitude (m/s)	—	$\mathcal{U}(58711, 59611)$	$\mathcal{U}(59047, 61047)$	—	—	—	—
e	Eccentricity	—	$\mathcal{U}(0, 170)$	$\mathcal{U}(0, 200)$	—	—	—	—
ω	Argument of periastron (degrees)	—	$\mathcal{U}(0, 1)$	$\mathcal{U}(0, 1)$	—	—	—	—
		—	$\mathcal{U}(0, 360)$	$\mathcal{U}(0, 360)$	—	—	—	—
Drift on SOPHIE:								
A	Linear RV drift (m/s)	—	—	—	$\mathcal{U}(-100.0, 100.0)$	—	—	—
Telescope Parameters:								
σ_{SOPHIE}	SOPHIE RV jitter (m/s)	$\mathcal{U}(1e-3, 200.)$	$\mathcal{U}(1e-3, 200.)$	$\mathcal{U}(1e-3, 200.)$	$\mathcal{U}(1e-3, 200.)$	$\mathcal{U}(1e-3, 100.)$	$\mathcal{U}(1e-3, 100.)$	$\mathcal{U}(1e-3, 200.)$
$\text{mu}_{\text{SOPHIE}}$	SOPHIE instrumental offset (m/s)	$\log \mathcal{U}(-50482, -50282)$	$\log \mathcal{U}(-38819, -38600)$	$\log \mathcal{U}(61489, 61689)$	$\log \mathcal{U}(-17000, -14500)$	$\log \mathcal{U}(-28557, -28357)$	$\log \mathcal{U}(70000, 80000)$	$\log \mathcal{U}(3925, 4125)$
σ_{HARPS}	HARPS RV jitter (m/s)	—	—	$\mathcal{U}(1e-3, 200.)$	—	—	—	—
mu_{HARPS}	HARPS instrumental offset (m/s)	—	—	$\log \mathcal{U}(61561, 61761)$	—	—	—	—
σ_{FEROS}	FEROS RV jitter (m/s)	—	—	$\mathcal{U}(1e-3, 200.)$	—	—	—	—
mu_{FEROS}	FEROS instrumental offset (m/s)	—	—	$\log \mathcal{U}(61528, 61728)$	—	—	—	—

Notes. The prior labels of \mathcal{U} and $\log \mathcal{U}$ indicate uniform, and uniform logarithms of distributions, respectively.

Table D.2: Adopted priors in joint modeling using EXOFASTv2. $\mathcal{N}[a, b]$ are Gaussian priors, where a and b are the mean and width, respectively.

Parameter	Units	TOI-1836	TOI-2295	TOI-2237	TOI-4081	TOI-4168	TOI-5076	TOI-5110
Stellar Parameters:								
M_*	Mass (M_\odot)	$\mathcal{N}[1.29, 0.08]$	$\mathcal{N}[1.17, 0.07]$	$\mathcal{N}[0.770, 0.05]$	$\mathcal{N}[1.44, 0.09]$	—	$\mathcal{N}[0.82, 0.05]$	$\mathcal{N}[1.46, 0.09]$
R_*	Radius (R_\odot)	$\mathcal{N}[1.611, 0.068]$	$\mathcal{N}[1.451, 0.061]$	$\mathcal{N}[0.774, 0.05]$	$\mathcal{N}[2.511, 0.105]$	—	$\mathcal{N}[0.798, 0.036]$	$\mathcal{N}[2.359, 0.099]$
T_{eff}	Effective Temperature (K)	$\mathcal{N}[6369, 153]$	$\mathcal{N}[5733, 138]$	$\mathcal{N}[4843, 153]$	$\mathcal{N}[6040, 145]$	—	$\mathcal{N}[4832, 119]$	$\mathcal{N}[6154, 148]$
[Fe/H]	Metallicity (dex)	$\mathcal{N}[-0.098, 0.08]$	$\mathcal{N}[0.316, 0.08]$	$\mathcal{N}[0.081, 0.08]$	$\mathcal{N}[0.0, 0.3]$	—	$\mathcal{N}[0.07, 0.06]$	$\mathcal{N}[0.067, 0.050]$
Planetary parameters:								
P	Period (days)	$\mathcal{N}[20.4, 0.1]$	$\mathcal{N}[30.0, 0.1]$	$\mathcal{N}[94.1, 0.5]$	$\mathcal{N}[9.3, 0.1]$	B	.01	$\mathcal{N}[30.1, 0.1]$
T_C	Time of conjunction ¹ (BJD _{TDB})	$\mathcal{N}[2459646.5, 0.1]$	$\mathcal{N}[2458713.5, 0.1]$	$\mathcal{N}[2458440.3, 0.5]$	$\mathcal{N}[2459736.331232, 0.1]$	—	$\mathcal{N}[23.4, 0.1]$	$\mathcal{N}[30.1, 0.1]$
R_p/R_*	Radius of planet in stellar radii	—	$\mathcal{N}[0.03, 0.21]$	—	—	—	$\mathcal{N}[60204, 0.0, 0.1]$	$\mathcal{N}[2459503.7, 0.1]$

Appendix E: Wavelength, telescope, and transit parameters derived from EXOFASTv2 fit

Table E.1: Wavelength, telescope, and transit parameters derived from EXOFASTv2 fit.

Parameter	Units	TOI-1836	TOI-2295	TOI-2237	TOI-4081	TOI-4168	TOI-5076	TOI-5110
Wavelength Parameters:								
u ₁ -TESS	linear limb-darkening coeff	0.217 ^{+0.029} _{-0.030}	0.326 ± 0.054	0.447 ^{+0.035} _{-0.036}	0.263 ^{+0.041} _{-0.040}	0.289 ^{+0.027} _{-0.019}	0.687 ± 0.051	0.241 ± 0.038
u ₂ -TESS	quadratic limb-darkening coeff	0.293 ± 0.033	0.276 ± 0.052	0.182 ± 0.033	0.303 ± 0.036	0.286 ^{+0.019} _{-0.020}	0.148 ^{+0.051} _{-0.052}	0.302 ± 0.036
u ₁ -CHEOPS							0.468 ^{+0.038} _{-0.037}	
u ₂ -CHEOPS							0.172 ^{+0.036} _{-0.037}	
A _b	Dilution from neighboring stars	—	—	—	0.0660 ± 0.0020	0.0231 ^{+0.0059} _{-0.0048}	—	—
Telescope Parameters:								
γ _{rel} -SOPHIE	Relative RV Offset (m/s)	-50381.5 ± 1.4	-38733.10 ^{+0.84} _{-0.81}	61596.8 ^{+8.3} ₋₁₂	-15016 ⁺²⁰ ₋₁₉	-29142 ⁺¹⁴ ₋₁₃	70291.5 ± 1.9	4012.2 ± 2.6
σ _J -SOPHIE	RV Jitter (m/s)	11.1 ^{+1.2} _{-1.1}	3.83 ^{+0.81} _{-0.69}	14.2 ^{+4.1} _{-3.8}	111 ⁺¹⁷ ₋₁₅	43 ⁺¹⁵ ₋₁₀	11.0 ^{+1.7} _{-1.4}	10.1 ^{+2.8} _{-2.3}
σ _J ² -SOPHIE	RV Jitter Variance (m/s)	124 ⁺²⁸ ₋₂₃	14.7 ^{+6.8} _{-4.8}	202 ⁺¹³⁰ ₋₉₄	12400 ⁺⁴²⁰⁰ ₋₃₀₀₀	1880 ⁺¹⁶⁰⁰ ₋₇₉₀	121 ⁺³⁹ ₋₂₈	102 ⁺⁶⁴ ₋₄₁
γ _{rel} -HARPS	Relative RV Offset (m/s)	—	—	61645.3 ^{+9.3} ₋₁₃	—	—	—	—
σ _J -HARPS	RV Jitter (m/s)	—	—	12.2 ^{+4.9} _{-4.5}	—	—	—	—
σ _J ² -HARPS	RV Jitter Variance (m/s)	—	—	148 ⁺¹⁴⁰ ₋₈₉	—	—	—	—
γ _{rel} -FEROS	Relative RV Offset (m/s)	—	—	61621 ⁺¹⁹ ₋₂₀	—	—	—	—
σ _J -FEROS	RV Jitter (m/s)	—	—	65 ⁺¹⁴ ₋₁₁	—	—	—	—
σ _J ² -FEROS	RV Jitter Variance (m/s)	—	—	4300 ⁺²¹⁰⁰ ₋₁₃₀₀	—	—	—	—
γ _{rel} -HARPS-N	Relative RV Offset (m/s)	—	—	—	—	—	—	—
σ _J -HARPS-N	RV Jitter (m/s)	—	—	—	—	—	70279.15 ± 0.49	—
σ _J ² -HARPS-N	RV Jitter Variance (m/s)	—	—	—	—	—	2.19 ^{+0.60} _{-0.58}	—
Transit Parameters:								
σ ² -FFI ¹	Added Variance	0.0126 ^{+0.0082} _{-0.0069}	—	see Table I.1	-0.086 ^{+0.011} _{-0.010}	—	0.0174 ^{+0.0035} _{-0.0034}	0.0217 ^{+0.0063} _{-0.0060}
F ₀ -FFI	Baseline flux	1.0002 ± 0.0036	—	see Table I.1	1.0002 ^{+0.0032} _{-0.0033}	—	1.0000 ± 0.0016	1.000069 ± 0.0000074
σ ² -2 minutes ¹	Added Variance	0.0229 ± 0.0059	0.0506 ± 0.0045	see Table I.1	-0.128 ± 0.032	—	0.00 ^{+0.0043} _{-0.0040}	0.604 ^{+0.029} _{-0.028}
F ₀ -2 minutes	Baseline flux	1.0002 ± 0.0012	1.0000 ± 0.0011	see Table I.1	1.0001 ± 0.0027	1.0000 ± 0.0016	1.0000 ± 0.0037	1.0000 ± 0.0017
σ ² -CHEOPS ¹	Added Variance	—	—	—	—	—	0.685 ^{+0.041} _{-0.038}	—
F ₀ -CHEOPS	Baseline flux	—	—	—	—	—	1.0004 ± 0.0020	—

Notes. ¹ Units are in ppm. The added variance might be a negative value to account for the overestimated photometric errors (Eastman et al. 2019)

Appendix F: Probability distribution function of TOI-2295b

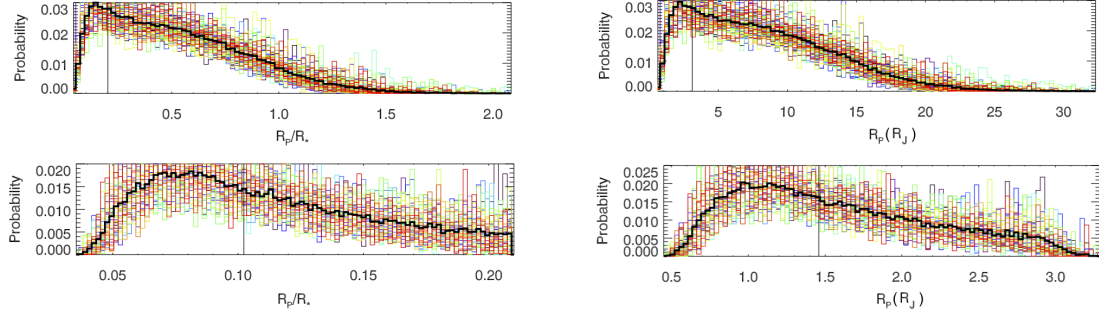


Fig. F.1: Probability distribution function for R_P/R_* and R_P for TOI-2295b, without applying prior on R_P/R_* (top) and with applying prior (bottom; see Sect. 4.2.1). Each color corresponds to an individual chain, with the thick black probability representing the average of all chains. The thin black vertical line indicates the median value.

Appendix G: Gaia mass constrain of TOI-2295c and TOI-2537c

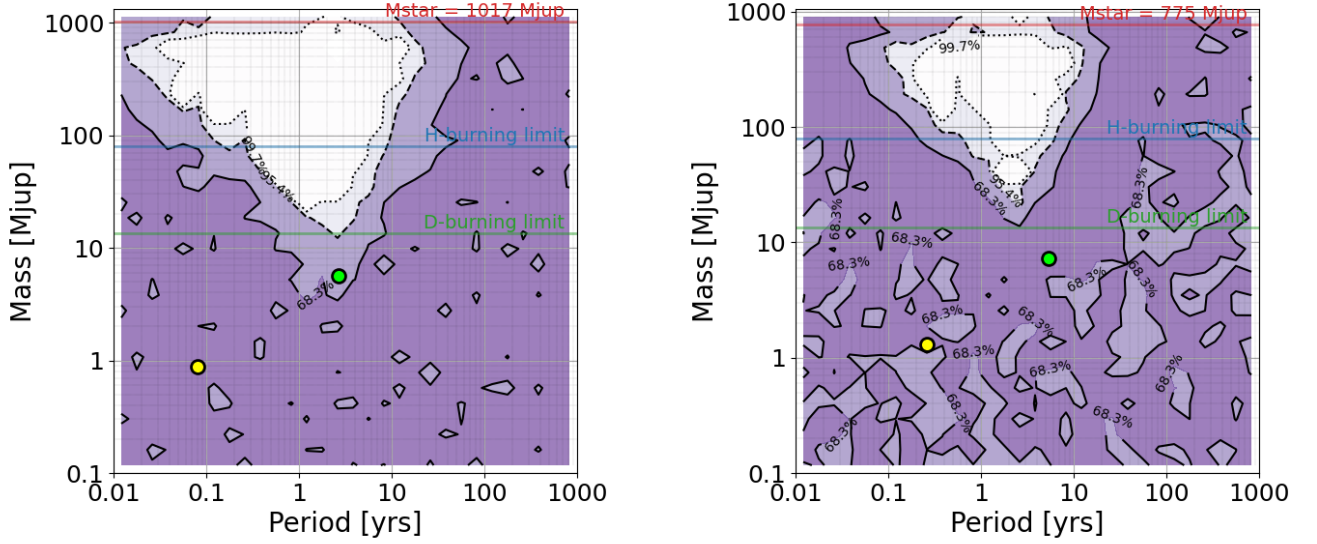


Fig. G.1: GaiaPMEX confidence map for the mass and orbital period of planets around TOI-2295 (left) and TOI-2537 (right), constrained by RUWE=0.919 and RUWE=1.06, respectively. The yellow and green circles indicate the mass and orbital period of planets b and c, respectively, as determined from the joint analysis.

Appendix H: RV residuals-bisector

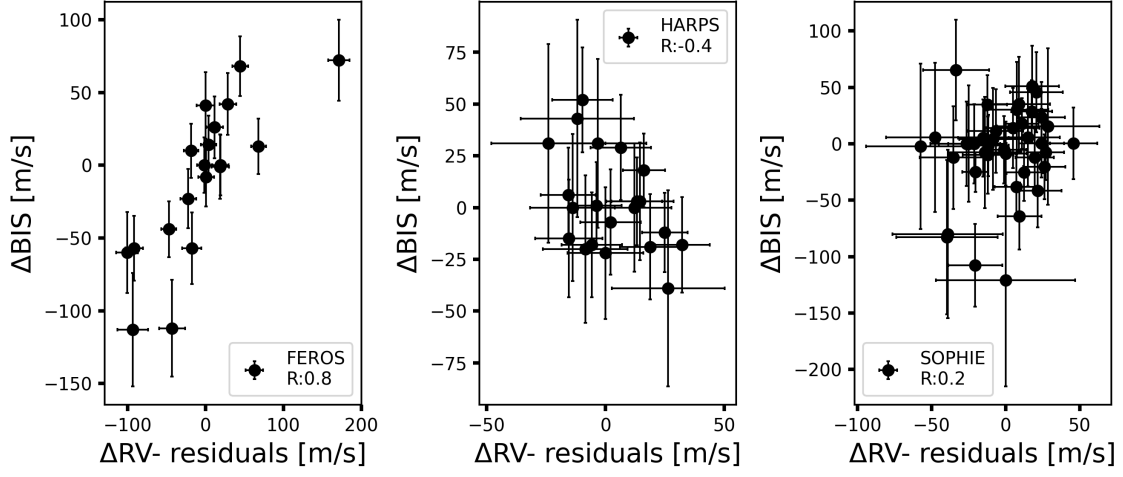


Fig. H.1: RV residuals after removing both planet signals versus bisectors for TOI-2537 data from FEROS, HARPS, and SOPHIE. The instrument names are indicated on the labels.

Appendix I: TTVs of TOI-2537b

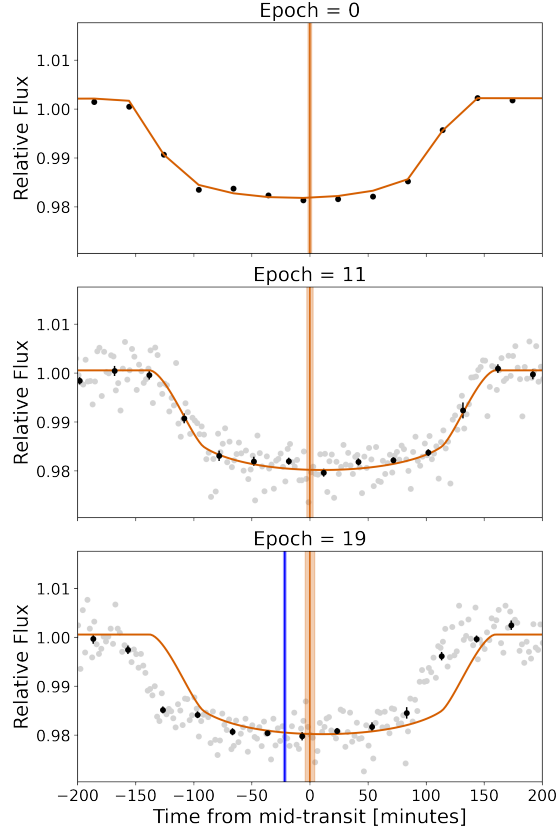


Fig. I.1: Individual TESS transit events of TOI-2537b. The model plotted here is fitted to the first two transits (shown in the *top* and *middle* panels) and is then used to estimate the model for the third detected transit (displayed in the *bottom* panel). Vertical orange lines indicate the predicted mid-transit times, along with their 1σ uncertainties, calculated using a linear ephemeris: $T_c = T_0 + E \times P$, where $T_0 = 2458440.3331 \pm 0.0011$ BJD is the time of conjunction at an arbitrary reference epoch, E is the epoch, and $P = 94.10245 \pm 0.00014$ d is the period. These T_0 and P values are derived from the fit to the first two transits. The vertical blue line represents the mid-transit time and its 1σ uncertainties measured by EXOFASTv2 for the *bottom* panel. The transit epochs are labeled at the top of each panel. This plot clearly illustrates the presence of TTVs. Unlike the current fit shown here, the model plotted in Fig. 7. and presented in Table. 7 accounts for TTVs.

Table I.1: Median values and 68% confidence intervals of the parameters for individual transits of TOI-2537 from the EXOFASTv2 fit.

Transit	Epoch	Mid-transit (BJD)	Added variance ¹ (σ^2)	Baseline flux (F_0)	TTV (min)
TESS UT 2018-11-17 (TESS)	0	2458440.3237 \pm 0.0011	$-0.094^{+0.071}_{-0.063}$	$1.0006^{+0.0054}_{-0.0055}$	-9.38 ± 2.16
TESS UT 2021-09-17 (TESS)	11	2459475.4661 \pm 0.0010	$-1.95^{+0.29}_{-0.28}$	$1.000554^{+0.000057}_{-0.000058}$	18.56 ± 2.35
TESS UT 2023-10-10 (TESS)	19	2460228.26460 \pm 0.00084	$-1.33^{+0.55}_{-0.51}$	1.00073 ± 0.00013	-7.69 ± 2.76

Notes. The TTV column shows the difference between the observed (third column) and predicted mid-transit times. The predicted mid-transit times are estimated using a linear ephemeris, with $T_0 = 2458440.3302 \pm 0.0010$ BJD and $P = 94.102091 \pm 0.000073$ d, which were obtained by minimizing the covariance between these two parameters. Further details of these calculations are provided in Sect. 18 of Eastman et al. (2019).¹ Units are in ppm. The added variance might be a negative value to account for the overestimated photometric errors (Eastman et al. 2019)